Electronic Materials Letters, Vol. 3, No. 4 (2007), pp. 185-189

The Effects of Various Purge Gasses on the Characteristics of $PbZr_xTi_{1-x}O_3$ Thin Films Prepared by Metalorganic Chemical Vapor Deposition

June Key Lee*

School of Materials Science and Engineering, Chonnam National University, 300 Yongbong, Gwangju 500-757, Korea

In order to optimize the metalorganic chemical vapor deposition process for $PbZr_xTi_{1-x}O_3$ (PZT) thin films, the effect of purge gas species was investigated. The two steps associated with the gas input process used for stabilizing reaction chamber pressure, viz. the gas flows prior to the deposition of the $PbTiO_3$ (PTO) seed layer and PZT thin film, respectively, were varied from N_2/O_2 = 0/2000sccm to N_2/O_2 = 2000/0sccm. The effects of these variations on the crystallinity and electrical properties of the PZT thin films were examined from the viewpoint of memory device applications. The properties of the PZT thin film exhibited remarkable dependency on the gas species before the deposition of the PTO seed layer, and insignificant dependency on the gas species before the deposition of the PZT film. The combination of a gas flow of N_2/O_2 = 500/1500sccm before the deposition of the PTO seed layer and of N_2/O_2 = 0/2000sccm before the deposition of the PZT film yielded a PZT thin film with the best properties, including high (111)-orientation (92.2%) and a high remnant polarization value ($2P_r$) of 71 μC/cm^2 at 3V. The retention property also showed strong dependency on the pre-deposition gas flow, in that 91.1% of the initial charge of the optimized sample could be maintained after 100 hours of baking at 150°C.

Keywords: PZT, PTO seed, MOCVD, retention, purge gas

1. INTRODUCTION

Since the 1960s, the promising properties of ferroelectric materials for applications involving nonvolatile memory devices have driven the intensive investigation of ferroelectric thin film technology. Current demand for portable equipment strongly requires the development of high-density ferroelectric random access memories (FRAM), because ferroelectric thin film can provide non-volatility, low power operation and high read/write speed[1]. Three materials, viz. $PbZr_xTi_{1-x}O_3$ (PZT), $SrBi_2Ti_2O_9$ (SBT) and $Bi_{4-x}La_xTi_3O_{12}$ (BLT), have been investigated intensively for the realization of FRAM devices. In this study, PZT was chosen as the ferroelectric material because it possesses a relatively low crystallization temperature (<600°C) and a large remnant polarization ($2P_r$ > 40 μC/cm^2)[2-4]. Various kinds of thin film deposition technology have been utilized to make PZT thin films, such as chemical solution deposition (CSD), sputtering, pulsed laser deposition (PLD), and metalorganic chemical vapor deposition (MOCVD)[3-8]. Among them, MOCVD promises to be the most practical technique for high-density FRAM integration because of multiple advantages such as a low deposition temperature, high growth rate, high uniformity, and high step coverage. According to the international technology roadmap for semiconductors (ITRS), the semiconductor industry expects that the MOCVD technique will be utilized for the integration of 256 Mbit density devices and beyond after 2010[9].

However, the PZT MOCVD process has a fundamental drawback, in that the stable delivery of metalorganic precursors is difficult to achieve with conventional bubbler technology, because of the lack of suitable precursors[10]. In order to overcome this limitation, the liquid source delivery (LSD) MOCVD technique was proposed and has shown promising results, although the high level of reproducibility required for mass production has yet to be achieved[3, 11-13]. MOCVD is a fairly complicated process, as it has many process parameters which must be controlled. Various methods have been used to improve the structural and electrical properties of PZT thin films, from varying process parameters such as the deposition temperature and the input amount and ratio of the precursors, to creative ideas such as seed layer and pulse-MOCVD[3, 14, 15]. In order to realize a reliable PZT MOCVD process, the effects of all possible process parameters must be deeply understood. In this study, we focused on the purge gas species that was supplied to stabilize the reaction chamber pressure prior to the deposition of the PZT thin film. In general, the effect of the purge gas species has been ignored,

*Corresponding author: junekey@chonnam.ac.kr

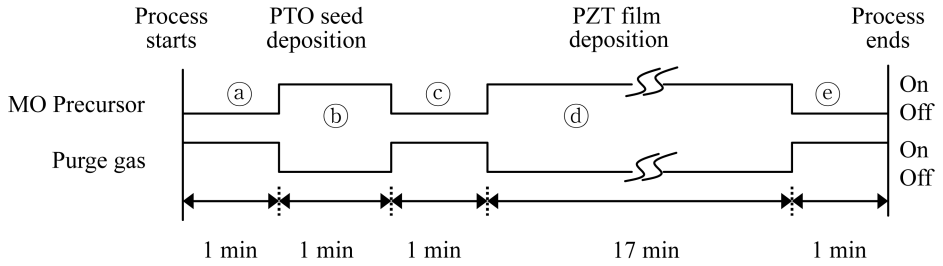

Fig. 1. Process sequence of the MOCVD process used for the deposition of the PZT thin film preparation. Step ⓑ corresponds to the deposition of the PTO seed layer, and step ⓓ to that of the PZT thin film. Steps ⓐ and ⓒ correspond to purge gas flows for 1 minute in order to stabilize the pressure in the reaction chamber.

because a chemically inert gas was utilized. However, if the purge gas interacts with the substrate, the initial state of the PZT MOCVD process could be substantially influenced, resulting in variation in the properties of the PZT thin film. In this study, the effect of the purge gas species was monitored in terms of the structural and electrical properties of the PZT thin films.

2. EXPERIMENTAL DETAILS

PZT thin film deposition was carried out in a Nexcap 2000 CVD reactor (Sunic System Ltd.). The showerhead technique was employed for the uniform deposition of a 6-inch wafer, and the liquid source delivery system was utilized in order to control the amount of precursor solutions supplied to the reactor with an accuracy of ±1%. The metalorganic precursors were $Pb(tmhd)_2$, $Zr(tmhd)_2(^iOPr)_2$ and $Ti(tmhd)_2(^iOPr)_2$, all of which were dissolved in octane solvent and reserved separately in each ampoule. PZT thin films were grown an Ir(100 nm)/Ti(5 nm) electrode, which was deposited on an SiO_2(200 nm)/Si(100) wafer at 200°C by DC magnetron sputtering. The deposition temperature of the PZT thin film was 530°C and the other major process parameters are described in references 4 and 14. The growth rate was about 6.0 nm/min, resulting in a PZT film thickness of about 100nm after a deposition time of 18 min. $PbTiO_3$ (PTO) with a thickness of 6 nm was utilized as a seed layer. Oxygen, nitrogen and a mixture of the two were utilized as purge gases with a total gas flow of 2000sccm.

A top Ir(70 nm)/IrO_2(30 nm) electrode was sputter-deposited and etched off to pattern capacitors with a size of $100 \times 100\ \mu m^2$ for the measurement of the electrical properties. The etching process was accomplished by inductively coupled plasma-reactive ion etcher (ICP-RIE). The structural properties were analyzed by X-ray diffraction (XRD) and X-ray photoelectron spectroscopy (XPS). The electrical properties were measured using a Radiant Technologies Precision Pro system.

3. RESULTS AND DISCUSSION

The MOCVD process used for the deposition of the PZT thin film consisted of five steps, as shown in Fig. 1. In this study, a 6 nm-thick PTO seed layer was deposited in order to reduce the deposition temperature of the PZT thin films[14, 16, 17]. There were two purge gas steps with a duration of 1 minute each prior to the deposition of the PTO seed layer and PZT thin film, respectively. In general, a chemically inert gas, such as nitrogen or argon, has been utilized as the purge gas for MOCVD. The main role of the purge gas is to stabilize the reaction chamber pressure, which could otherwise be perturbed by the sudden supply of metalorganic precursors at the initial stage of film growth. Conventionally, N_2 was utilized as the purge gas for the PZT MOCVD process, but it was replaced with O_2 in this work. Interestingly, the hysteretic property was greatly improved, in that the remnant polarization ($2P_r$) value was drastically increased to 62 μC/cm² as compared with the value of $2P_r = 34\ \mu C/cm^2$ when N_2 was used as the purge gas, as shown in Fig. 2. Since the iridium (Ir) electrode can be oxidized in O_2 ambient, the initial stage of PTO seed growth might be seriously influenced by

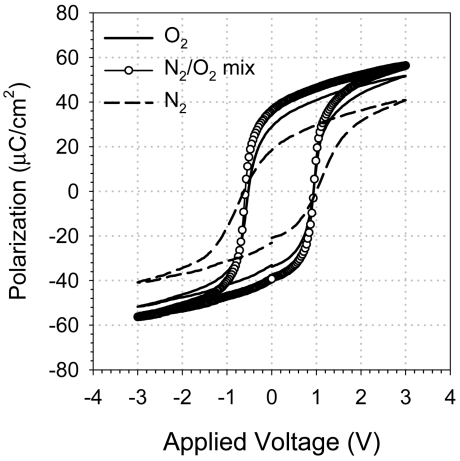

Fig. 2. Ferroelectric hysteresis loops for the Ir/IrO_2/PZT/Ir capacitors fabricated using three different purging gases for the deposition of the PTO seed layer (step ⓐ). The gas flow ratio in step ⓒ was fixed at N_2/O_2 = 0/2000sccm. Line (—) : O_2 2000sccm, dashed line (---) : N_2 2000sccm, circle (○) : N_2/O_2 = 500/1500sccm. The remnant polarization values ($2P_r$) are 62μC/cm² (—), 34 μC/cm² (---), and 71 μC/cm² (○).

the purge gas species during step ⓐ. Once again, N_2 was added to the O_2 purge gas and the effect was evaluated in terms of the hysteretic property of the resulting film. The $2P_r$ value increased with an increasing amount of N_2 and the optimum value (71 μC/cm^2) was observed at a mixture ratio of N_2/O_2 = 500/1500sccm. Fig. 3 shows an X-ray diffraction θ-2θ scan analysis, which indicates that the crystal structure of the PZT thin films is heavily dependant on the purge gas species. FRAM chip makers have endeavored to achieve highly (111)-oriented PZT thin films because they exhibit a higher $2P_r$ value and improved retention properties [18]. However, unlike CSD-derived PZT thin films that are highly (111)-oriented, MOCVD PZT thin films usually show a predominantly (100) or (001)-textured structure with some (101), (110) and (111)-type orientation, or a polycrystalline structure without any preferred orientation, when they are deposited at low temperature [4, 15, 18, 19]. A (111) preferred orientation has also been reported with MOCVD PZT, but only at a high deposition temperature of more than 590°C [3, 20]. It was revealed in this study that the orientation of the PZT thin film could be controlled by simply altering the purge gas species, as shown in Fig. 3. At an optimized purge gas flow, that is N_2/O_2 = 500/1500sccm, the PZT thin film displayed 92.2% (111)-orientation with 5.1% (100) and 2.7% (101)-orientation, as shown in Table 1. When the proportion of N_2 exceeded the optimized condition, the XRD peak intensity *I(111)* and $2P_r$ values gradually decreased, ultimately leading to the deposition of a PZT thin film with a highly (100) preferred orientation.

After step ⓐ, the process was stopped and the Ir electrodes were pulled out for surface analysis. An XPS analysis was attempted in order to investigate the difference in the surface state when the Ir electrodes were exposed to O_2, N_2, and mixtures of the two gases. However, no differences were observed in the XPS analysis. We took out the PTO seed layer after step ⓑ, and reattempted the XPS analysis. In Fig. 4, the peak shift of the Ti *2p* peak to a lower binding energy of about 0.5 eV was observed when the purge gas was pure N_2. The peak synthesis indicated that about 60% of the Ti

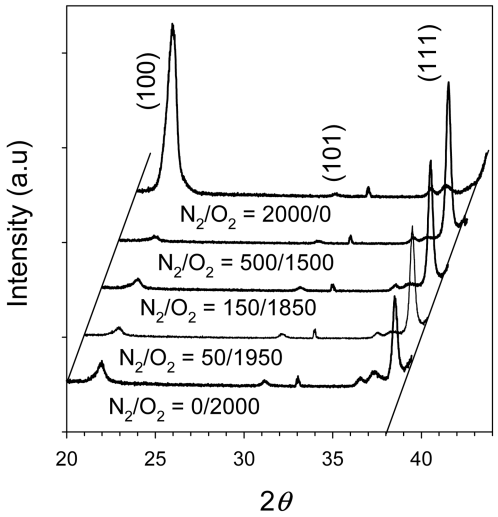

Fig. 3. X-ray diffraction θ-2θ pattern of the PZT thin films deposited with various purging gas mixture ratios prior to the deposition of the PTO seed layer. The purge gas in step ⓒ was fixed at N_2/O_2 = 0/2000sccm.

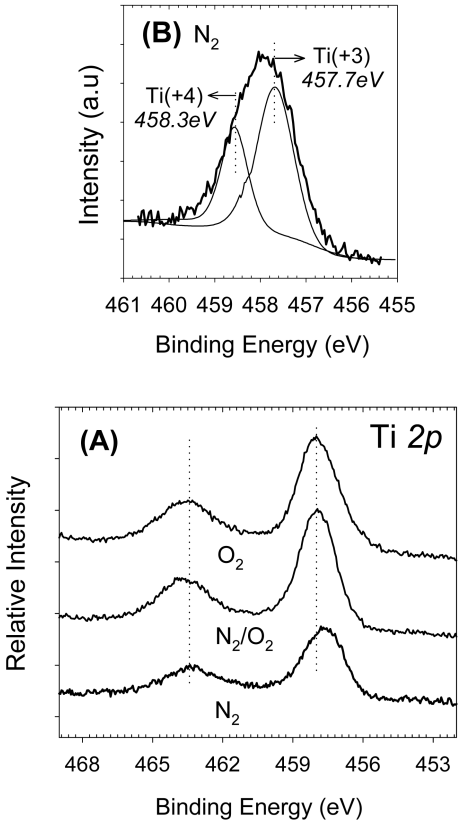

Fig. 4. XPS analysis of Ti elements in PTO seed layer deposited with three different purge gases in the first purge step ⓐ. In the case of the N_2 purge gas, the Ti *2p* peak was shifted to a lower binding energy (A). The peak synthesis indicates that about 60% of the Ti is in the partially oxidized Ti(+3) state (B).

Table 1. Ratio of XRD peak intensity as a function of the purging gas (N_2/O_2) flow rate in step ⓐ. The purge gas in step ⓒ was fixed at N_2/O_2 = 0/2000sccm. *I(ijk)* (%) = *I(ijk)*/[*I(100)*+*I(101)*+*I(111)*] × 100

N_2/O_2 flow (sccm)	0/2000	50/1950	150/1850	500/1500	2000/0
I(100) (%)	19.9	13.2	9.5	5.1	90.9
I(101) (%)	6.9	6.4	4.0	2.7	3.4
I(111) (%)	73.2	80.4	86.5	92.2	5.7

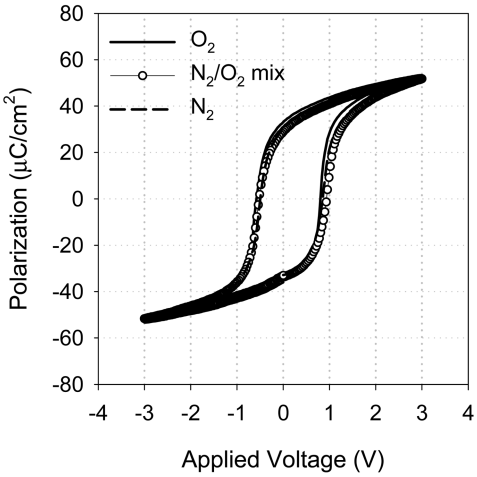

Fig. 5. Ferroelectric hysteresis loops for the Ir/IrO_2/PZT/Ir capacitors fabricated using three different purging gases for the deposition of the PZT film (step ⓒ). Line (—) : O_2 2000sccm, dashed line (---) : N_2 2000sccm, circle (○) : N_2/O_2 = 500/1500sccm. The remnant polarization values ($2P_r$) are 62 μC/cm^2 (—), 56 μC/cm^2 (---), and 58μC/cm^2 (○). The purge gas in step ⓐ was fixed at N_2/O_2 = 0/2000sccm.

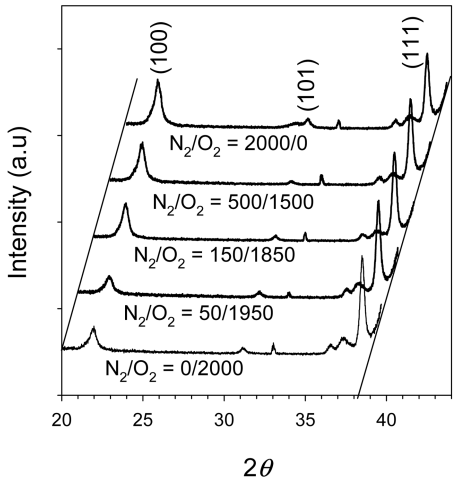

Fig. 6. X-ray diffraction θ-2θ pattern of the PZT thin films deposited with various purging gas mixture ratios prior to the deposition of the PZT thin film in step ⓒ . The purge gas in step ⓐ was fixed at N_2/O_2 = 0/2000sccm.

was in the partially oxidized Ti(+3) state. This observation could not directly explain the PZT crystal orientation hereafter, but proved that the purge gases do affect the initial state prior to the growth of the PZT thin films.

The influence of the purge gas species during step ⓒ was examined with the same approach as that used for step ⓐ. On the basis of the shapes of the hysteresis curve, the effect of the purge gas species was found to be insignificant, as shown in Fig. 5. The PZT thin film capacitors exhibited $2P_r$ values within the range of 56 - 62 μC/cm^2 depending on the purge gas mixing ratio. A systematic trend was observed wherein there was an increase in the (111)-orientation as the proportion of O_2 in the purge gas was increased (Fig. 6 and Table 2). In accordance with the previous results, the highly (111)-oriented PZT thin films displayed larger $2P_r$ values.

With the optimized purge gas conditions in step ⓐ and step ⓒ, that is N_2/O_2 = 500/1500sccm for the deposition of the PTO seed layer and N_2/O_2 = 0/2000sccm for that of the PZT thin film, the PZT thin film capacitor showed excellent resistance against the retention test, as shown in Fig. 7. After baking for 100 hr at 150°C, the PZT thin film capacitor maintained about 91.1% of its initial switching charge under the optimized condition, while the use of the O_2 and N_2 purging conditions resulted in initial switching charges of 83.6% and 54.9%, respectively. This might be due to the fact that the highly (111)-oriented PZT film allows for simple domain switching movement.

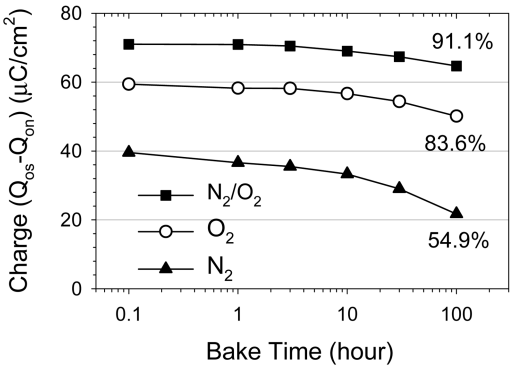

Fig. 7. Retention properties of the Ir/IrO_2/PZT/Ir capacitors fabricated using the three different purging gases for the deposition of the PTO seed layer. The gas flow ratio in the second purge step ⓒ was fixed at N_2/O_2 = 0/2000sccm. The baking temperature is 150°C and the hysteresis properties were measured at 85°C. Circle (○) : O_2 = 2000sccm, triangle (▲) : N_2 = 2000sccm, square (■) : N_2/O_2 = 500/1500sccm.

In this study, it was found that the purge gas species could significantly influence the structural and electrical properties of PZT thin films in the MOCVD process. For the MOCVD

Table 2. Ratio of XRD peak intensity as a function of the purging gas (N_2/O_2) flow rate in step ⓒ . The purge gas in step ⓐ was fixed at N_2/O_2 = 0/2000sccm. *I(ijk)* (%) = *I(ijk)*/[*I(100)*+*I(101)*+*I(111)*] × 100

N_2/O_2 flow (sccm)	0/2000	50/1950	150/1850	500/1500	2000/0
I(100) (%)	19.9	21.7	28.2	32.3	36.5
I(101) (%)	6.9	7.0	5.7	4.4	8.7
I(111) (%)	73.2	71.3	66.1	63.3	54.8

of PZT thin films with high remnant polarization and (111)-orientation, it is recommended that an optimized N_2 and O_2 mixture should be employed as the purge gas.

4. CONCLUSIONS

100 nm-thick PZT thin films were prepared on an Ir electrode by liquid delivery MOCVD with a 6 nm-thick PTO seed layer. The PZT films were deposited at 530°C and the effect of the purge gas was investigated in detail. In the study of the purge gas flow prior to the deposition of the PTO seed layer, as the proportion of N_2 in the purge gas increased, the crystal (111)-orientation and remnant polarization values were linearly increased. When only N_2 was employed, the PZT film showed a highly (100)-orientation and a small remnant polarization value. On the other hand, in the study of the purge gas flow prior to the deposition of the PZT film, the effect of the gas flow ratio was insignificant, although a linear trend was observed wherein the (111)-orientation was increased as the proportion of N_2 in the purge gas decreased.

Under the optimized conditions, namely a purge gas flow of N_2/O_2 = 500/1500sccm before the deposition of the PTO seed layer, and N_2/O_2 = 0/2000sccm before the deposition of the PZT film, the PZT thin film showed high (111)-orientation (92.2%), a remnant polarization value of 71 μC/cm^2 and a coercive voltage of 0.72V at 3V. The retention property also showed a strong dependency on the purge gas species in that, under the optimized conditions above, 91.1% of the initial charge was maintained after 100 hours of baking at 150°C.

ACKNOWLEDGEMENTS

This work was supported by a Korea Research Foundation Grant funded by the Korean Government (MEHERD, Basic Research promotion Fund) under contract number KFR-2005-003-D00140). June Key Lee is especially grateful to the research fund of the MOCIE (Ministry of Commerce, Industry and Energy) for the support provided under contract number 10024488.

REFERENCES

1. G. Muller, T. Happ, M. Kund, G. Y. Lee, N. Napal, and R. Sezi, *IEDM Tech. Dig.* p. 567 (2004).
2. Chi Kong Kwak and S. B. Desu, *J. Mater. Res*. **9**, 1728 (1994).
3. S. R. Gilbert, S. Hunter, D. Ritchey, C. Chi, D. V. Taylor, J. Amano, S. Aggarwal, T. S. Moise, T. Sakada, S. R. Summerfelt, K. K. Singh, C. Kazemi, D. Carl, and B. Bierman, *J. Appl. Phys*. **93**, 1713 (2003).
4. J. K. Lee, M. Lee, S. Hong, W. Lee, Y. K. Lee, S. Shin, and Y. Park, *Jpn. J. Appl. Phys*. Pt 1, **41**, 6690 (2002).
5. G. Yi, Z. Wu, and M. Sayer, *J. Appl. Phys*. **64**, 2717 (1998).
6. A. Croteau, S. Matsubara, Y. Miyasaka, and N. Shohara, *Jpn. J. Appl. Phys*. **26**, 18 (1987).
7. S. B. Krupanidhi, H. Hu, and V. Kumar, *J. Appl. Phys*. **71**, 376 (1992).
8. J. S. Horowitz, K. S. Grabowski, K. B. Chrisey, and R. E. Leuchtner, *Appl. Phys. Lett*. **59**, 1565 (1991).
9. International Technology Roadmap for Semiconductor, 2005 ed.
10. A. C. Jones, T. J. Leedham, P. J. Wright, M. J. Crosbie, D. J. Williams, H. O. Davies, K. A. Fleeting, P. O'Brien, and M. E. Pemble, *Mater. Sci. Semicond. Processing* **2**, 165 (1999).
11. A. C. Jones, T. J. Leedham, P. J. Wright, D. J. Williams, M. J. Crosbie, H. O. Davies, K. A. Fleeting, and P. O'Brien, *J. Eur. Ceram. Soc*. **19**, 1431 (1999).
12. S. Chen, J. F. Roeder, T. E. Glassman, and H. Baum, *Chem. Mater*. **11**, 209 (1999).
13. J. H. Park, H. J. Joo, S. K. Kang, Y. M. Kang, H. S. Rhie, B. J. Koo, S. Y. Lee, B. J. Bae, J. E. Lim, H. S. Jeong, and Kimam Kim, *IEDM Tech. Dig*. p. 591 (2004).
14. Youngsoo Park, June Key Lee, Yong Kyun Lee, Ilsub Chung, Jung Soo Yong, and Young Ho Park, *Integrated Ferroelectrics* **39**, 231 (2001).
15. M. Aratani, K. Nagashima, and H. Funakubo, *Jpn. J. Appl. Phys*. Pt 1, **40**, 4126 (2001).
16. C. K. Kwok and S. B. Desu, *J. Chem. Res*. **8**, 339 (1993).
17. S. Hiboux and P. Muralt, *J. Eur. Ceram. Soc*. **24**, 1593 (2004).
18. D. J. Jung, S. Y. Lee, B. J. Koo, Y. S. Hwang, D. W. Shin, J. W. Lee, Y. S. Chun, S.H. Shin, M. H. Lee, H. B. Park, S. I. Lee, K. Kim, and J. G. Lee, *VLSI Tech. Symp*. p. 122 (1998).
19. Seung-Hyun Kim, Chang Young Koo, Dong-Yeon Park, Dong-Su Lee, Jung-Hoon Yeom, and Jowoong Ha, *J. Kor. Phy. Soc*. **42**, S1417 (2003).
20. M. De Keijser, G. J. M. Dormans, P. J. Van Veldhoven, and P. K. Larson, *Integr. Ferroelectr*. **3**, 243 (1993).